

Supporting information

Trifunctional Metal-Organic Platform for Environmental Remediation: Structural Features With Peripheral Hydroxyl Groups Facilitate Adsorption, Degradation and Reduction

Harpreet Kaur,^a Rakesh Kumar,^a Ajay Kumar,^a Venkata Krishnan^{a*} and Rik Rani Koner^{b*}

^a*School of basics Sciences, Indian Institute of Technology Mandi, Mandi-175001,HP India.*

^b*School of Engineeing, Indian Institute of Technology Mandi, Mandi-175001,HP India.*

S. No	Contents	No.
1	Synthesis scheme of Cd-MOF	Figure S1
2	Crystal data and structure refinement for Cd-MOF	Table S1
3	Photographs showing a color change of different dyes during adsorption and separation study using Cd-MOF	Figure S2 (a, b)
4	Packing diagram of Cd complex along a-axis.	Figure S3
5	SEM and TEM images of Cd -MOF	Figure S4 (a-d)
6	N ₂ Adsorption isotherm and Pore size distribution graph for Cd-MOF	Figure S5 (a, b)
7	DRS spectra of Cd-MOF	Figure S6 (a, b)
8	UV-vis spectra of adsorption study of RhB and MO using Cd-MOF up to 24 h	Figure S7

9	UV-vis spectra of pH dependent adsorption study of MB dye using Cd-MOF	Figure S8
10	Comparison of MB adsorption capacity with various other reported MOF materials	Table S2
11	Pseudo-second- order kinetics parameters for MB dye adsorbed into Cd-MOF	Table S3
12	Langmuir model for MB dye adsorption into Cd-MOF	Table S4
13	% Adsorption capacity of MB dye using Cd-MOF in three successive cycles of adsorption-desorption experiment.	Figure S9
14	XRD patterns of Cd-MOF before and after MB dye adsorption	Figure S10
15	SEM and TEM images of recovered Cd-MOF after MB dye adsorption	Figure S11
16	UV-Vis spectra of RhB dye degradation using recovered Cd-MOF.	Figure S12
17	UV-vis spectra for photocatalytic reduction of Cr(VI) during different amount of EtOH, UV-vis spectra of photocatalytic Cr(VI) reduction with addition of AgNO ₃ and without addition of AgNO ₃	Figure S13(a-f)
18	SEM and TEM images of recovered Cd-MOF after photocatalytic Cr(VI) reduction	Figure S14

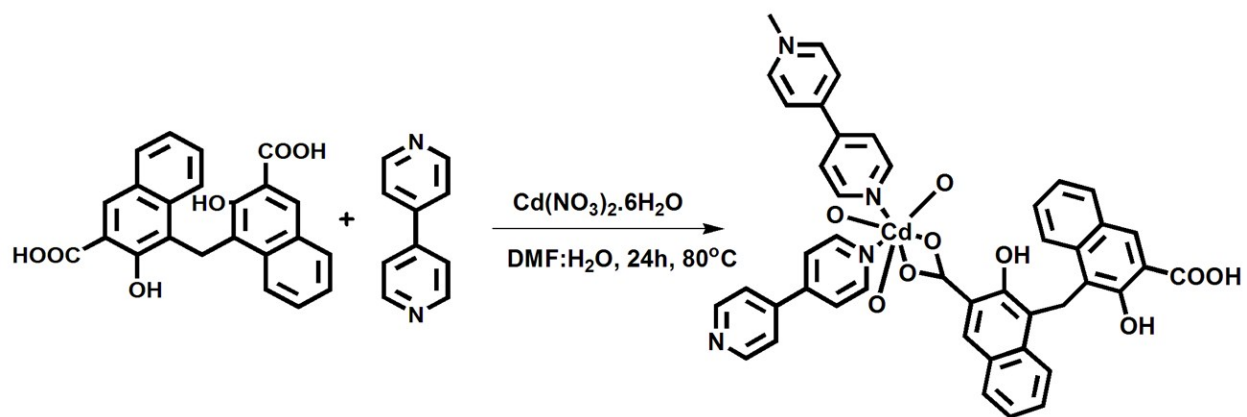


Figure S1. Synthesis scheme of Cd-MOF.

Table S1. Crystal data and structure refinement for Cd-MOF.

1.	Identification code	Cd-MOF
2.	Emperical Formula	$\text{C}_{43}\text{H}_{30}\text{CdN}_4\text{O}_6$
3.	Formula weight	811.11
4.	Temperature/K	293 (2)
5.	Crystal System	monoclinic
6.	Space group	$\text{P2}_1/\text{c}$
7.	Unit Cell dimensions	$a/\text{\AA} = 13.6269 (3), b/\text{\AA} = 16.8816 (4),$ $c/\text{\AA} = 19.4131 (5)$ $\alpha/^\circ = 90.00, \beta/^\circ = 107.141(3), \gamma/^\circ = 90.00$
8.	Volume/ \AA^3	4267.52 (19)

9.	Z	4
10.	$\rho_{\text{calc}} \text{ g/cm}^3$	1.262
11.	$\mu \text{ mm}^{-1}$	4.490
12.	F(000)	1648.0
13.	Crystal size/ mm^3	$0.247 \times 0.147 \times 0.111$
14.	2 θ range for data collection/ $^\circ$	7.08 to 133.86
15.	Index ranges	$-16 \leq h \leq 15, -19 \leq k \leq 13, -23 \leq l \leq 22$
16.	Reflection collected	15192
17.	Independent reflections	7484 [$R_{\text{int}} = 0.0279, R_{\text{sigma}} = 0.0350$]
18.	Goodness-of-fit on F^2	1.078
19.	Final R indexes[$I > 2\sigma(I)$]	$R1 = 0.0331, wR2 = 0.0889$
20.	Final R indexes(all data)	$R1 = 0.0384, wR2 = 0.0945$
21.	Largest diff. peak/ hole/e \AA^3	0.80/ -0.49

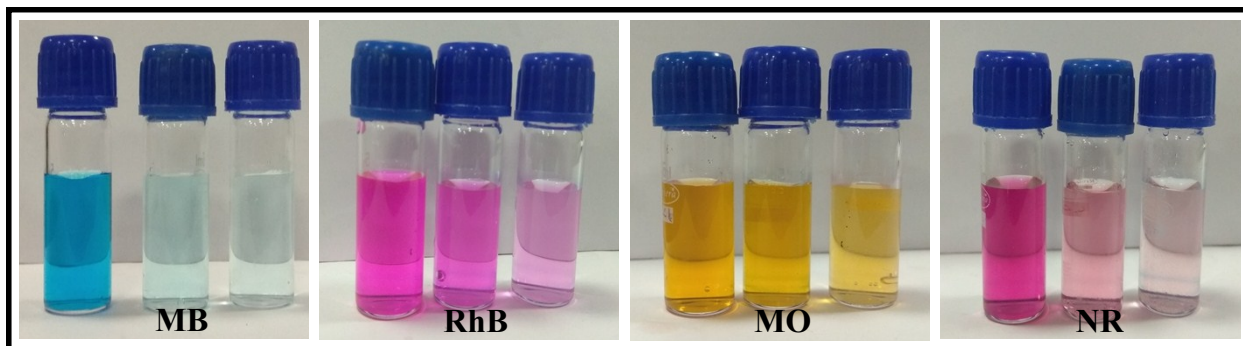


Figure S2. (a) Photographs showing a color change of different dyes during adsorption study using Cd-MOF.

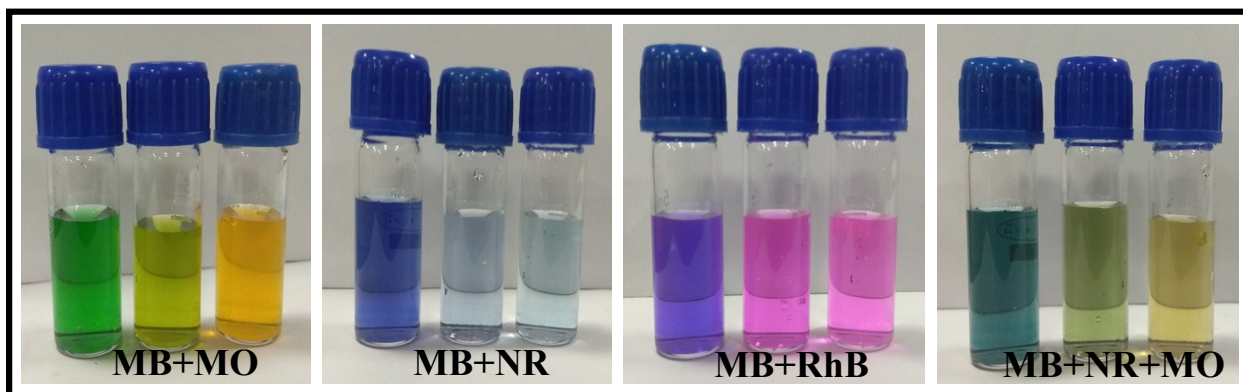


Figure S2. (b) Photographs showing color change during separation study of a mixture of two dyes (a: MB+MO, b: MB+NR, c: MB+RhB) and three dyes (d: MB+NR+MO) using Cd-MOF.

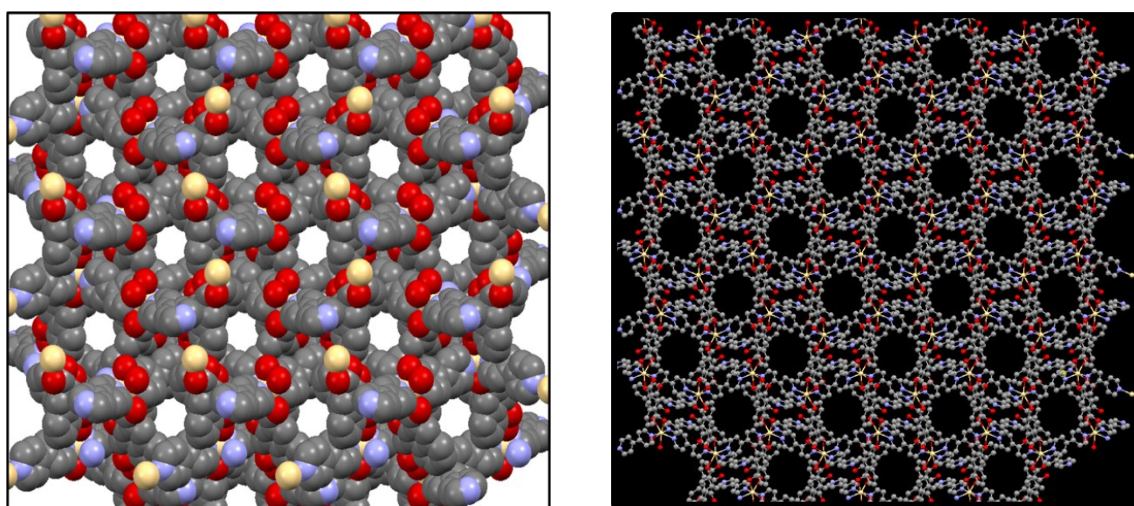


Figure S3. Packing diagram of Cd complex along a-axis.

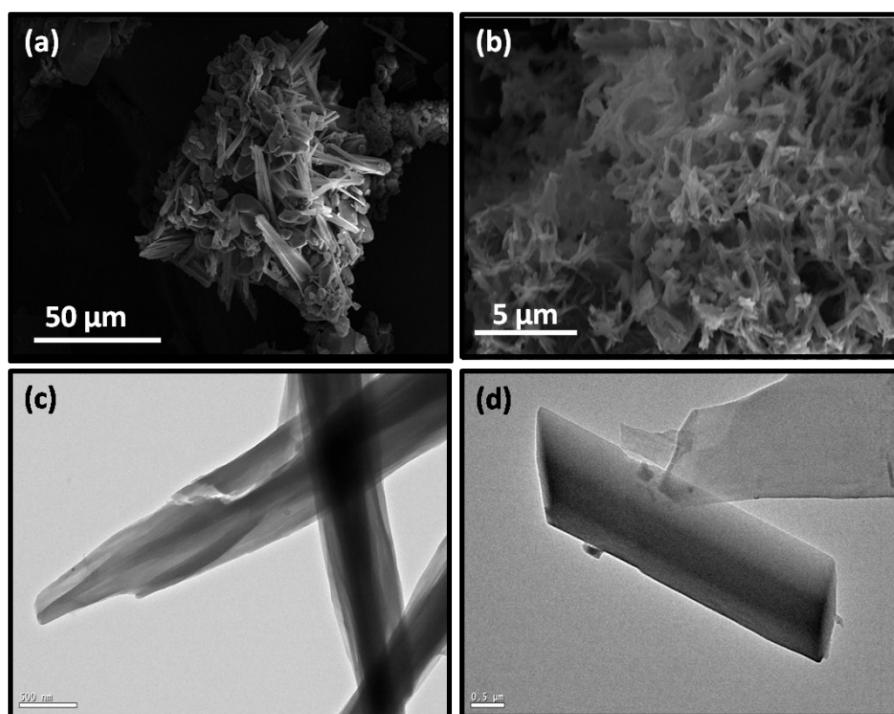


Figure S4. SEM images (a, b) and TEM images (c, d) of Cd-MOF.

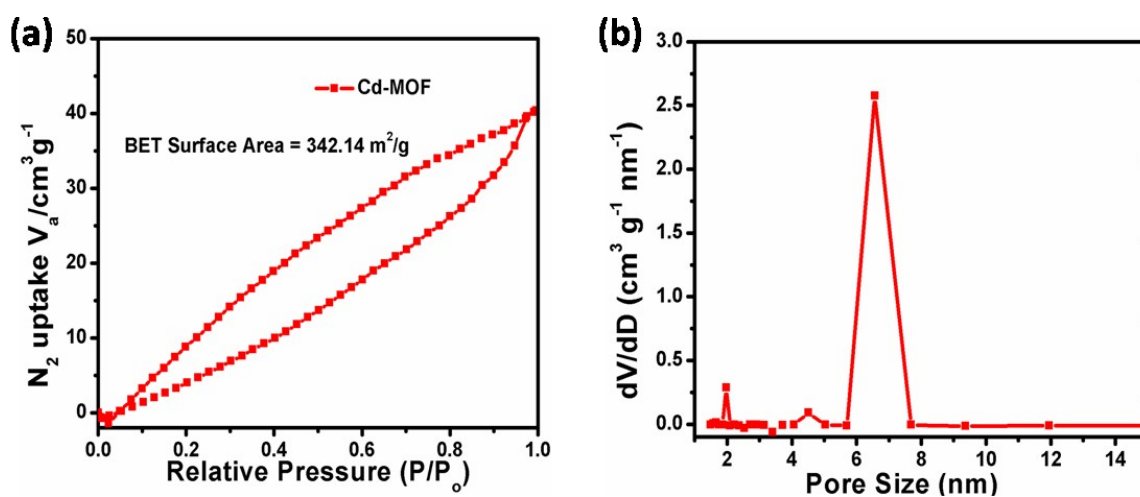


Figure S5. (a) N_2 adsorption isotherms of Cd-MOF. (b) Pore size distribution graph. On the basis of N_2 adsorption studies, BET surface area for Cd-MOF at 77K was found to be $342.14 \text{ m}^2 \text{ g}^{-1}$ and pore radius = 17.585 \AA .

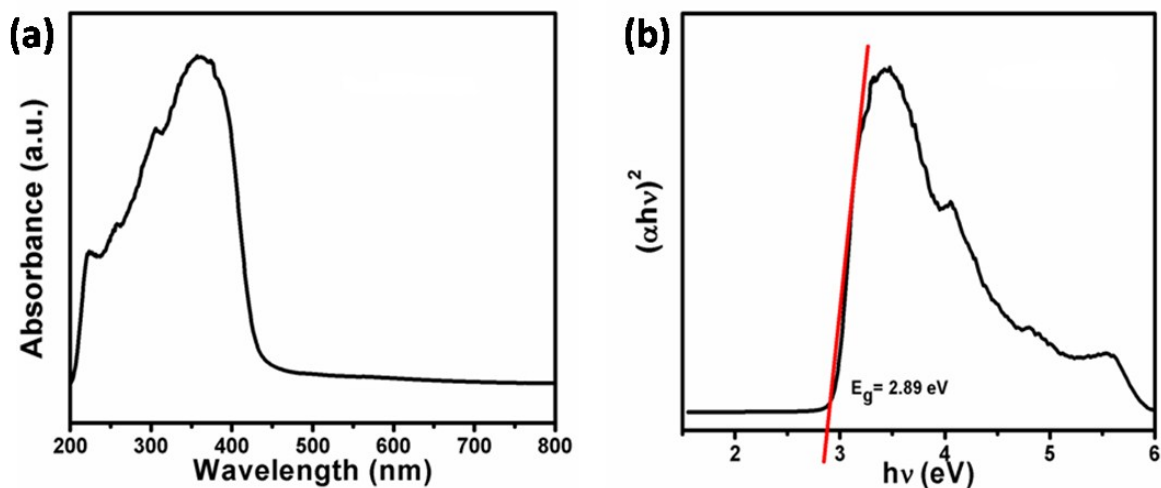


Figure S6. (a) Absorption spectra of Cd-MOF. (b) Plot showing transformed Kubelka–Munk function vs. energy of light for the band gap.

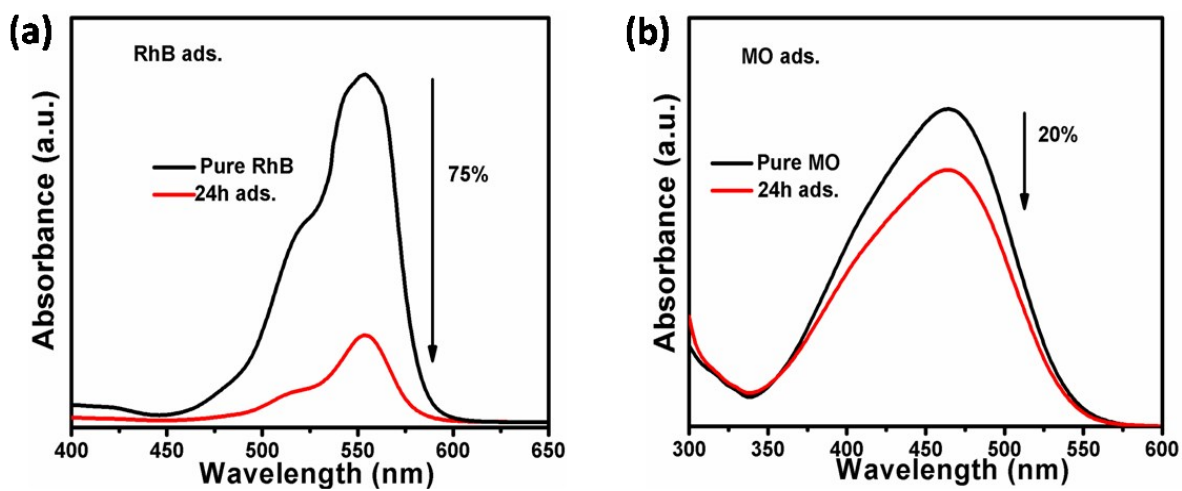


Figure S7. UV-vis spectra for the adsorption study of (a) RhB and (b) MO dye using Cd-MOF upto 24 h.

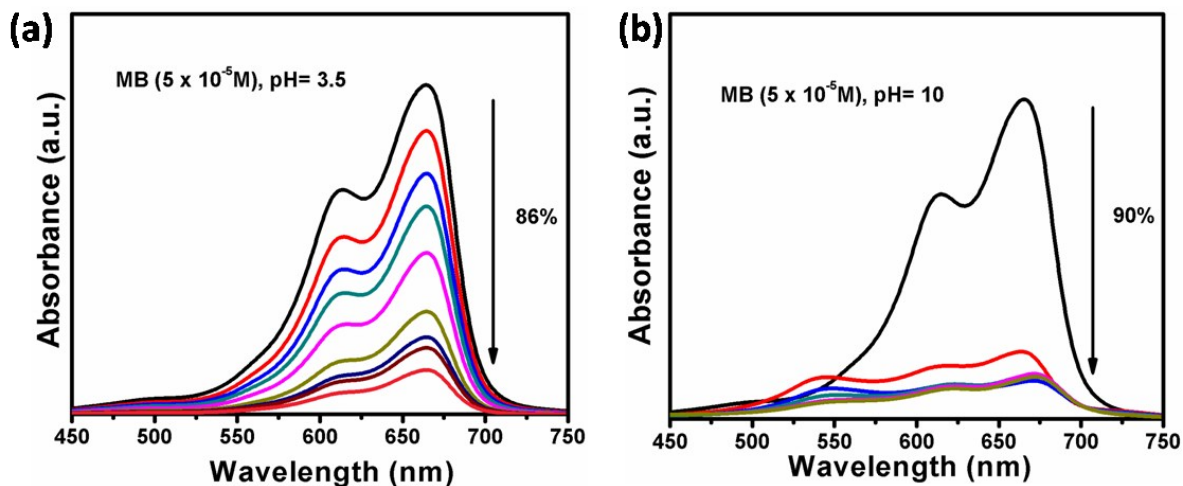


Figure S8. UV-vis spectra of pH dependent adsorption study of MB dye using Cd-MOF.

Table S2. Comparison of MB adsorption capacity with various other reported MOF materials.

Material	%Adsorption/ Adsorption Capacity	Time	Ref.
$[\text{Cd}_3(\text{tib})_2(\text{BTB})_2] \cdot 3\text{DEF} \cdot 4.5\text{H}_2\text{O}$	69%	24 h	Y.-L. Li, Y. Zhao, P. Wang, Y.-S. Kang, Q. Liu, X.-D. Zhang and W.-Y. Sun, <i>Inorg. Chem.</i> , 2016, 55, 11821-11830.
$[\text{Cd}_3(\text{tib})_2(\text{BTB})_2(\text{DMA})_2(\text{H}_2\text{O})_2] \cdot 2\text{DMA} \cdot 8\text{H}_2\text{O}$	55%		
$\{[\text{Cd}_2(\text{BPTC})(\text{DMA})_2(\text{DMPU})_5(\text{H}_2\text{O})_5](\text{DMPU})_5\}_n$	25mg/g	24 h	W.-J. Ji, R.-Q. Hao, W.-W. Pei, L. Feng and Q.-G. Zhai, <i>Dalton Trans.</i> , 2018, 47, 700-707.
$[\text{Co}_3(\text{tib})_2(\text{BPT})_2(\text{H}_2\text{O})_2] \cdot \text{DMA} \cdot 2.5\text{H}_2\text{O}$	0.6×10^{-3} mg/g	24 h	Y.-L. Li, Y. Zhao, Y.-S. Kang, X.-H. Liu and W.-Y. Sun, <i>Cryst. Growth Des.</i> , 2016, 16, 7112-7123.
$[\text{Co}_3(\text{tib})_2(\text{BTB})_2] \cdot 2\text{DMF} \cdot 6\text{H}_2\text{O}$	6.4×10^{-3} mg/g		
$[\text{Cu}_{24}(\text{5-hip})_{24}(\text{bpy})_6(\text{H}_2\text{O})_{12}]$	0.546 mmol/g	48 h	H.-N. Wang, F.-H. Liu, X.-L. Wang, K.-Z. Shao and Z.-M. Su, <i>J. Mater. Chem. A</i> , 2013, 1, 13060-13063

$[(\text{CH}_3)_2\text{NH}_2]_2[\text{ZnNa}_2(\mu\text{-H}_2\text{O})_2(\text{H}_2\text{O})_2(\text{TATAT})].2\text{DMF}$	0.75 mg/g	-	C. Y. Sun, X. L. Wang, C. Qin, J. L. Jin, Z. M. Su, P. Huang and K. Z. Shao, Chem. Eur. J., 2013, 19, 3639-3645
$[\text{Cd}_6(\text{L})_2(\text{bib})_2(\text{DMA})_4]$	30 mg/g	72 h	F. Y. Yi, J. P. Li, D. Wu and Z. M. Sun, Chem. Eur. J., 2015, 21, 11475-11482.
$[(\text{C}_2\text{H}_5)_2\text{NH}_2]_2[\text{Mn}_6(\text{L})(\text{OH})_2(\text{H}_2\text{O})_6].4\text{DEF}$	67.5%	96 h	Y.-C. He, J. Yang, W.-Q. Kan, H.-M. Zhang, Y.-Y. Liu and J.-F. Ma, J. Mater. Chem. A, 2015, 3, 1675-1681.
$\{[\text{Cd}(\text{PA})(4,4'\text{-bpy})_2](\text{H}_2\text{O})\}_n$	29.60 mg/g	2 h	Present work

Table S3. Pseudo-second-order kinetics parameters for MB dye adsorbed into Cd-MOF.

Adsorbent	q_e (mg g ⁻¹)	K_2 (h g mg ⁻¹)	R^2
Cd-MOF	6.66	0.085	0.997
	9.99	0.068	0.995
	13.33	0.031	0.994
	16.66	0.200	0.997
	33.33	0.137	0.999

Table S4. Langmuir model for MB dye adsorption into Cd-MOF.

Adsorbent	Dye	K_L (L mg ⁻¹)	q_m (mg g ⁻¹)	R^2
Cd-MOF	MB	0.51	47.05	0.997

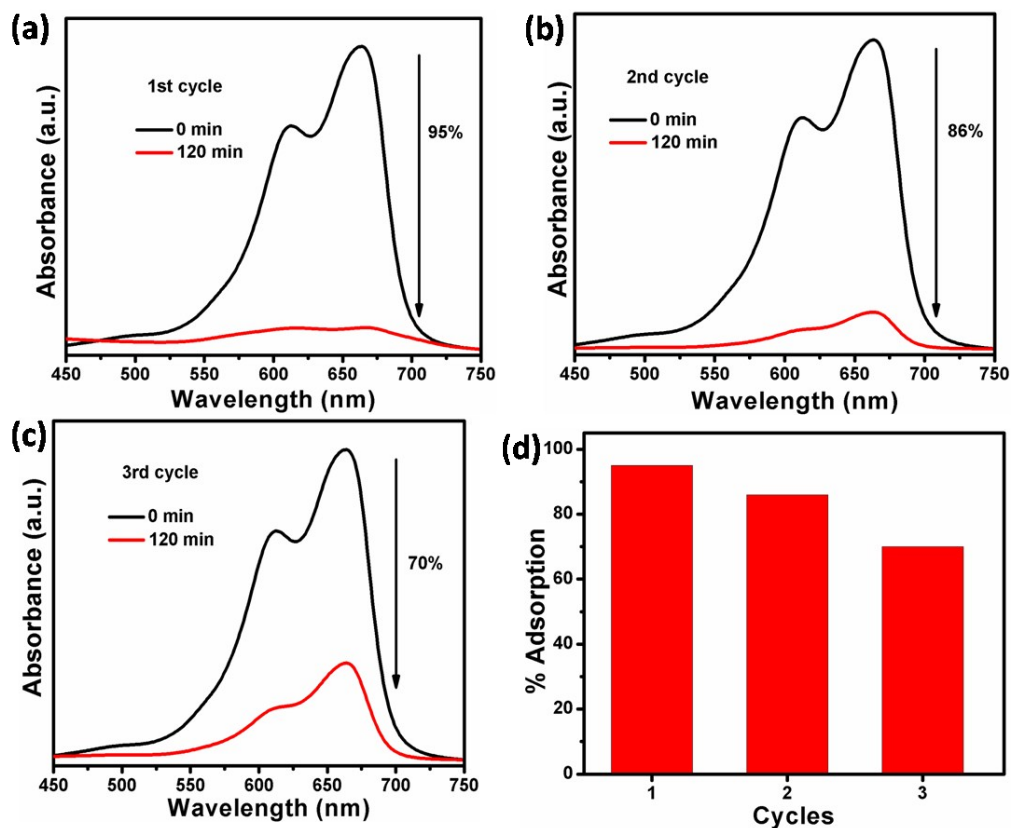


Figure S9. Adsorption capacity (%) of MB dye using Cd-MOF in three successive cycles of adsorption-desorption experiment (a to c). (d) Histogram for adsorption (%) of MB dye in adsorption-desorption experiment using Cd-MOF.

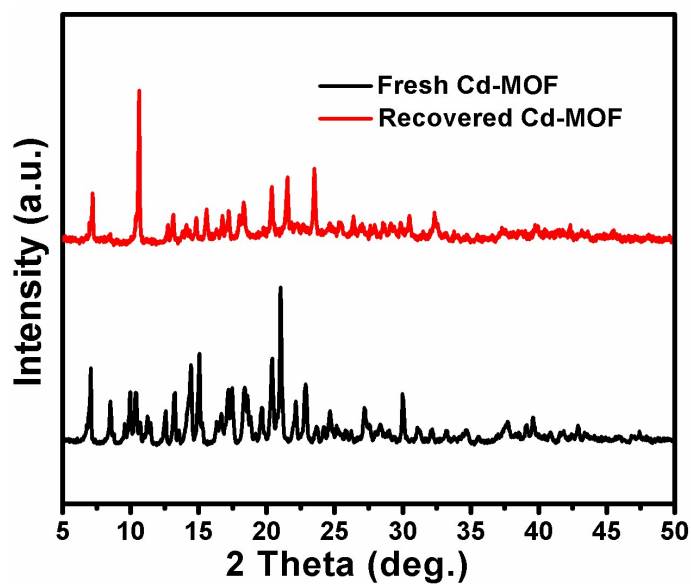


Figure S10. XRD patterns of Cd-MOF before and after MB dye adsorption.

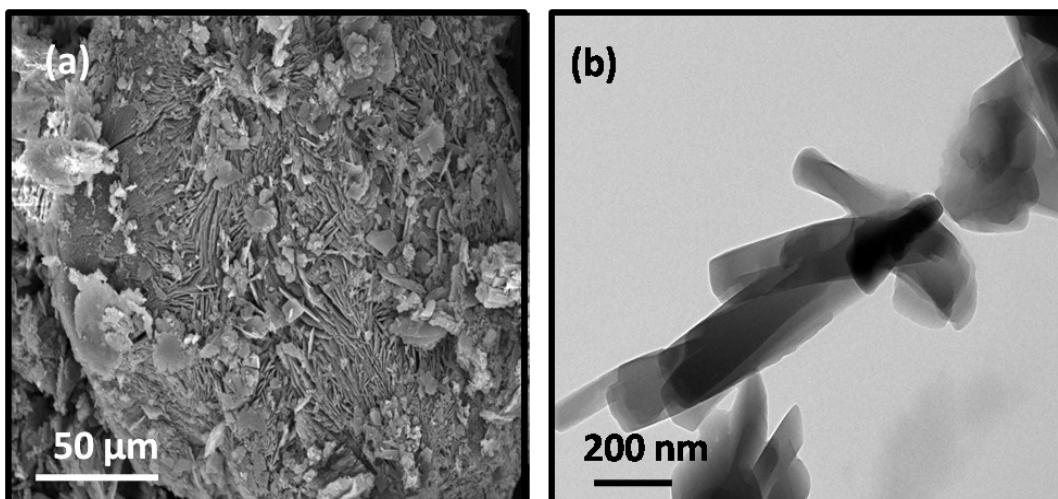


Figure S11. (a) SEM and (b) TEM images of recovered Cd-MOF after MB dye adsorption.

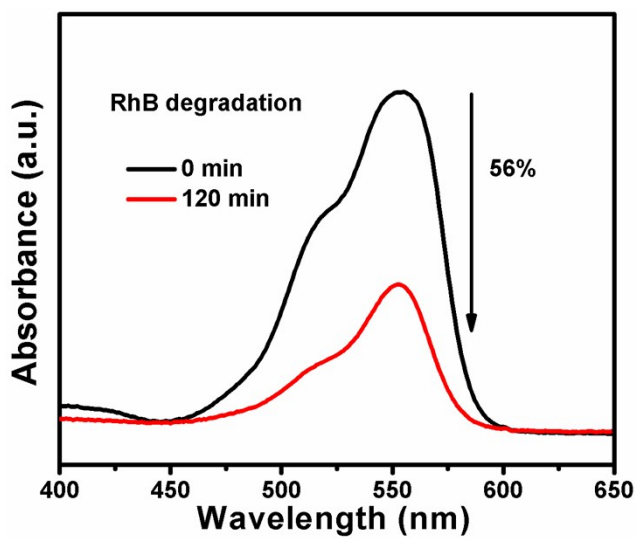


Figure S12. UV-Vis spectra of RhB dye degradation using recovered Cd-MOF.

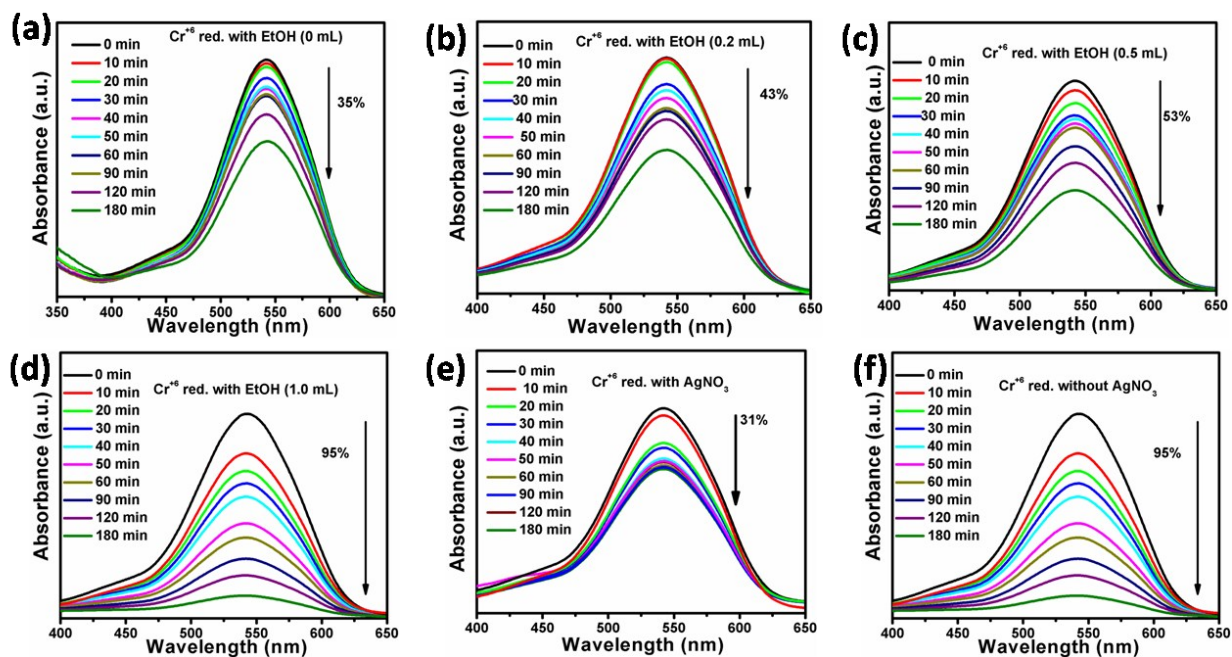


Figure S13. UV-vis spectra for photocatalytic reduction of Cr(VI) during different amount of EtOH (a to d). UV-vis spectra of photocatalytic Cr(VI) reduction. (e) with addition of AgNO_3 . (f) without addition of AgNO_3 .

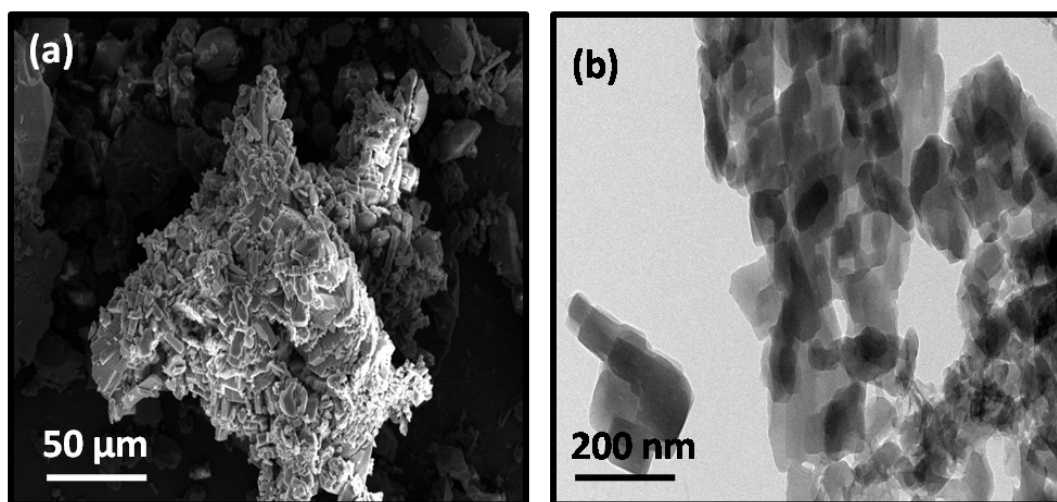


Figure S14. (a) SEM and (b) TEM images of recovered Cd-MOF after photocatalytic Cr(VI) reduction.